JMEPEG (2006) 15:218-222
DOI: 10.1361/105994906X95913

A Study of Diamond Synthesis by Hot Filament Chemical Vapor Deposition on Nc Coatings

R. Polini, S. Kumashiro, M.J. Jackson, M. Amar, W. Ahmed, and H. Sein

(Submitted November 4, 2005; in revised form December 27, 2005)

Deposition of diamond films onto various substrates can result in significant technological advantages in terms of functionality and improved life and performance of components. Diamond is hard, wear resistant, chemically inert, and biocompatible. It is considered to be the ideal material for surfaces of cutting tools and biomedical components. However, it is well known that diamond deposition onto technologically important substrates, such as co-cemented carbides and steels, is problematic due to carbon interaction with the substrate, low nucleation densities, and poor adhesion. Several papers previously published in the relevant literature have reported the application of interlayer materials such as metal nitrides and carbides to provide bonding between diamond and hostile substrates. In this study, the chemical vapor deposition (CVD) of polycrystalline diamond on TiN/SiN$_x$ nc (nc) interlayers deposited at relatively low temperatures has been investigated for the first time. The nc layers were deposited at 70 or 400 °C on Si substrates using a dual ion beam deposition system. The results showed that a preliminary seeding pretreatment with diamond suspension was necessary to achieve large diamond nucleation densities and that diamond nucleation was larger on nc films than on bare sc-Si subjected to the same pretreatment and CVD process parameters. TiN/SiN$_x$ layers synthesized at 70 or 400 °C underwent different nanostructure modifications during diamond CVD. The data also showed that TiN/SiN$_x$ films obtained at 400 °C are preferable in so far as their use as interlayers between hostile substrates and CVD diamond is concerned.

Keywords chemical vapor deposition (CVD), diamond, nc, superhard coatings, TiN/Si$_3$N$_4$

1. Introduction

The extreme hardness, high thermal conductivity, chemical inertness, and remarkable wear resistant properties make diamond one of the most technological and scientifically valuable materials found in nature (Ref 1). To deposit quality adherent diamond films on technologically important materials such as Co-cemented tungsten carbide (WC-Co) and high-speed steel (HSS) is highly desirable both in research and industrial applications. However, direct diamond film chemical vapor deposition (CVD) onto WC-Co and ferrous alloys is proving to be problematic due to the strong interaction between the carbon-containing gas phase and the substrate at the high CVD temperatures necessary to grow polycrystalline diamond films with large phase purity (Ref 2-6). Interdiffusion processes between the gas phase and the substrate can lead to carbon dissolution into transition metals (Co, Ni, Fe), as well as cementite (Fe$_3$C) formation. Both these effects cause significant metallurgical modifications of the substrate material and suppress diamond nucleation. In addition, transition metals with a partially filled *3d* shell also catalyze the formation of sp^2 carbon at the substrate/diamond interface, with deleterious effects on films adhesion (Ref 7). Moreover, the large differences in thermal expansion coefficients of ferrous alloys and diamond cause large compressive stresses at the diamond/steel interface that lead to film delamination when cooling from the relatively high diamond CVD temperatures to room temperature. One way of improving the nucleation and adhesion of the diamond film is to use a diffusion barrier layer between the substrate material and the film. This layer should be an effective barrier against diffusion of carbon into the substrate, accommodate the thermally induced stresses developed during the growth stage and ramp down process, and be of adequate thickness and morphology (Ref 8-10). Endler et al. (Ref 11) have investigated the use of TiN and Si$_3$N$_4$ interlayers on high speed steel to overcome these problems. There are still complications caused by the lack of adhesion and uniformity of diamond film nucleation.

Since the first attempts by Li and co-workers (Ref 12) to increase the hardness of TiN by adding Si, it has been recently shown by Veprek's group that nc-TiN/a-Si$_3$N$_4$ deposited by plasma-induced CVD could exceed 80 GPa hardness (Ref 13). These multiphase nc coatings consist of nanocrystalline TiN embedded in an amorphous matrix of silicon nitride, providing outstanding hardness and high oxidation resistance. Because these properties are important in high-load/high-temperature applications, these materials could also be potentially useful as interlayers for high-temperature diamond CVD on hostile substrates. In this paper, the first report on the behavior of TiN/SiN$_x$ nc coatings is provided when subjected to diamond CVD.

2. Experimental Procedures

A dual ion bean source was used to deposit 0.2 μm thin nc TiN/SiN$_x$ interlayers onto sc-Si wafers. In this system atoms

---

This paper was presented at the fourth International Surface Engineering Congress and Exposition held August 1-3, 2005 in St. Paul, MN.

R. Polini and **S. Kumashiro,** Dipartimento di Scienze e Tecnologie Chimiche, Università di Roma Tor Vergata, Via della Ricerca Scientifica, 00133 Rome, Italy; **M.J. Jackson,** Birck Nanotechnology Center, Purdue University, West Lafayette, IN 47907; and **M. Amar, W. Ahmed,** and **H. Sein,** Department of Chemistry and Materials, Manchester Metropolitan University, Chester Street, Manchester M1 5GD, U.K. Contact e-mail: jacksomj@purdue.edu.

Table 1 Nc TiN/SiN$_x$ deposition parameters

	nc70	nc400
Target	**Ti/Si**	
Base pressure	2.7×10^{-6} torr	
Reactive gas	N_2	
Sputtering gas	Ar	
Temperature	70 °C	400 °C
Beam energy	600 eV	
Si content at.%	8.7	
Ti:Si:N ratio	$Ti_{0.38}Si_{0.087}N_{0.533}$	
Ion to atom ratio	1:1	
Deposition time	120 min	

are sputtered by one ion beam while a second ion beam is used for energy assistance. The ion beam approach has the advantages of providing excellent control of deposition parameters, removal of residual gases and other contaminants from the substrate, transfer of additional energy to surface, and depositing atoms, which give more surface mobility and allow atoms to move to different sites producing denser and better bonded films and allowing film stress to change, usually from tensile to compressive (Ref 14). The use of nc coatings on Si substrates was investigated as potential barrier layers for diamond film nucleation and growth on hostile substrates. The nc layers were deposited at two different substrate temperatures (70 and 400 °C). These two interlayers, which will be referred to in the text as nc70 and nc400, were prepared according to the deposition parameters listed in Table 1 with the properties characterized by Rutherford backscattering (RBS). Prior to diamond deposition, several substrates were ultrasonically treated for 10 min with a 0.25 μm diamond powder suspension (DP-Suspension HQ, by Struers, Ballerup, Denmark). This treatment, usually referred to as "seeding," facilitates enhanced diamond nucleation either by implanting tiny diamond fragments into the substrate surface onto which diamond can subsequently grow during CVD (Ref 15), or by creating suitable defects at the substrate surface, which favor the heterogeneous nucleation of diamond from the gas phase (Ref 16). Diamond deposition was carried out using the hot-filament CVD (HFCVD) reactor previously described (Ref 17). In Table 2, the diamond deposition parameters are reported. All samples were characterized by field emission scanning electron microscopy (FE-SEM, Leo Supra 35) and by x-ray diffraction techniques (XRD, Philips X'Pert-Pro, Cu Kα radiation, $\lambda = 1.5418$ Å, graphite filtered). The measurements were done at glancing incidence where the angle between the x-ray beam and the surface of the film was kept constant (1°). Particle sizes were evaluated by means of the Scherrer equation, $D = K\lambda\nu(\beta \cos \theta)$, after Warren's correction for instrumental broadening. In this equation, D is the mean crystallite diameter of the supposedly spherical particles, K is a constant, equal to 0.9 rad, λ is the wavelength of the x-ray used (1.5418 Å), β is the effective line width of the x-ray reflection under observation (calculated using $\beta^2 = B^2 - b^2$, where B is the full width at half-maximum (FWHM)), b is the instrumental line broadening, and θ is the diffraction angle. To better estimate the position and the FWHM of XRD peaks, XRD spectra were submitted to a deconvolution procedure using the Peak Fitting module of Origin Pro 7 (by OriginLab Corporation), using pseudo-Voigt functions.

Table 2 Diamond deposition conditions

Operating parameters	Operating conditions
CH_4/H_2 volume ratio	1.0 vol.%
Total gas pressure	4.8 kPa
Total flow rate	300 sccm
Filament/substrate distance	8 mm
Filament temperature	2150-2200 °C
Substrate temperature	650-700 °C
Deposition time	4 h

3. Experimental Results and Discussion

3.1 Nc70

Figure 1 shows the high-resolution SEM image of a virgin nc70 film on Si. TiN particles embedded in the amorphous silicon nitride matrix were clearly detectable, with dimensions in the 10 to 20 nm range. Figure 2 shows the XRD spectra of both virgin and diamond CVD nc70 samples. The sharp peaks at around 55° are attributable to the substrate. The spectrum of the virgin TiN/SiN$_x$ coating showed, besides substrate peaks, the presence of only one phase. This phase can be assigned to the cubic NaCl structure, typical for TiN (JCPDS card no. 38-1420) (Ref 18), with a lattice parameter of approximately 0.430 nm. The TiN crystals in nc films prepared at 70 °C exhibited a (111) preferred orientation, as witnessed by the scarcely visible (200) reflection (this should be the most intense XRD peak of TiN), and the higher intensity of the (111) reflection, whose broadening confirmed the nanostructure of the TiN phase. In fact, the FWHM of the (111) peak, after correction for instrumental line broadening, was 1.44°, which allowed an average TiN particle size of 18.5 nm to be calculated. This is in good agreement with FE-SEM observation (Fig. 1).

Both the lattice parameter and the (111) preferred orientation confirmed the findings of Rebouta et al. (Ref 19) with respect to Ti-Si-N film growth prepared by DC reactive magnetron sputtering, with low (<10 at.%) Si levels.

The predominant (111) texture of TiN particles was still present after diamond deposition (Fig. 2). The corrected FWHM was 1.25°, corresponding to an estimated average particle size of 21 nm. The XRD data showed that the position of the TiN (111) peaks was shifted to 36.86°, corresponding to a lattice parameter of 0.422 nm, which is in agreement, within the experimental error, with the value expected for an unstressed lattice (0.424 nm). These findings indicated that Ostwald ripening of TiN particles was negligible and that the original stress state of TiN was relaxed after 4 h of diamond CVD at 650 to 700 °C.

The XRD spectra of samples subjected to diamond deposition showed that more abundant diamond formation occurred on samples, which were seeded prior to CVD. In fact, the (111) and (220) diamond peaks were clearly detectable after diamond CVD only for seeded samples. The XRD characterization was confirmed and clarified by SEM observations. Figure 3 shows the low-magnification SEM image of both seeded and unseeded nc70 samples subjected to diamond CVD. The positive effect of seeding on diamond nucleation was clearly evident. The surface of the interlayer that underwent to the seeding treatment prior to diamond CVD was almost entirely covered by diamond, and this clarifies the larger intensities of diamond XRD peaks observed for the seeded samples. Figure 4 shows the surface morphology of the unseeded low-temperature (70 °C)

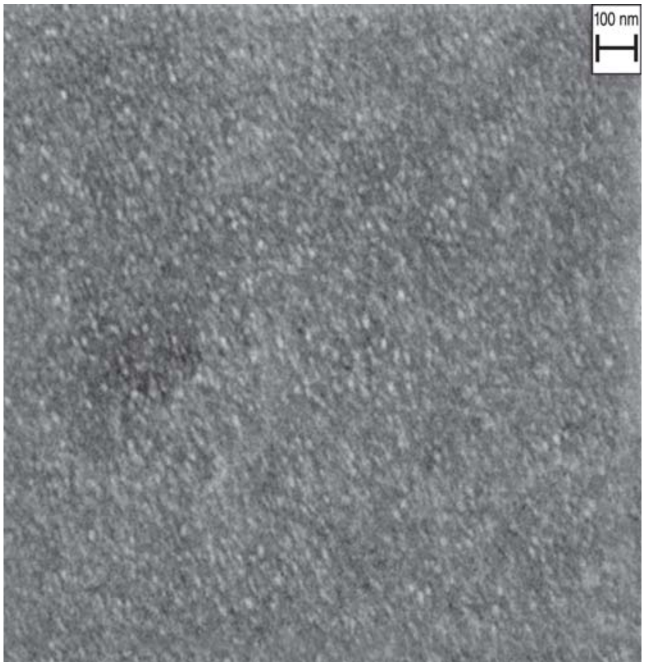

Fig. 1 FE-SEM image of TiN/SiN$_x$ nc film deposited on sc-Si at 70 °C

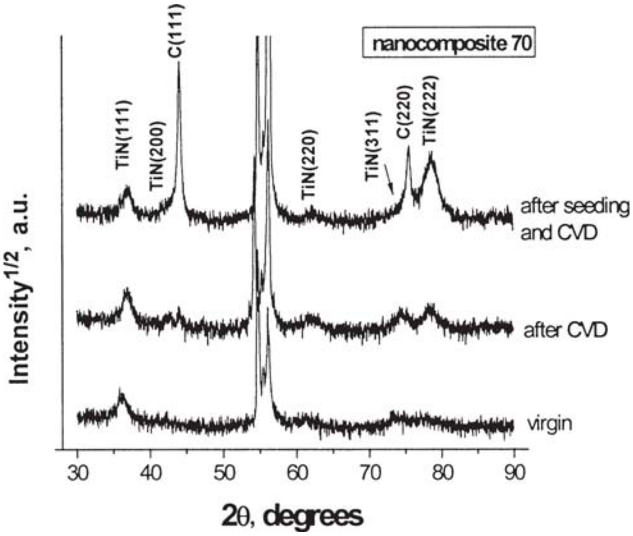

Fig. 2 Low-angle XRD spectra of nc films grown on sc-Si at 70 °C before (virgin) and after diamond CVD

nc interlayer after diamond CVD. It was quite evident that delamination of the interlayer occurred. This fact can be ascribed to the large stresses the interlayer (formerly grown at 70 °C) underwent when heated from room temperature up to the diamond deposition temperature (around 700 °C). The thermal expansion coefficient (TEC) of Ti-Si-N nc coatings is expected to be intermediate between the one of TiN (9.35×10^{-6} K^{-1}) and the one of the amorphous silicon nitride matrix (whose value could range from 1.19×10^{-6} K^{-1} for β-Si$_3$N$_4$ to 3.89×10^{-6} K^{-1} for *c*-Si$_3$N$_4$ at room temperature), and therefore, significantly larger than silicon's TEC (2.49×10^{-6} K^{-1}). Thus, delamination was most likely caused by the large TEC mismatch at the two different deposition temperatures. The same delamination was observed for samples subjected to seeding prior to CVD in correspondence of substrate areas, which were not covered by diamond. The interlayer detachment could also be responsible for the TiN stress relaxation after diamond CVD as detected by XRD.

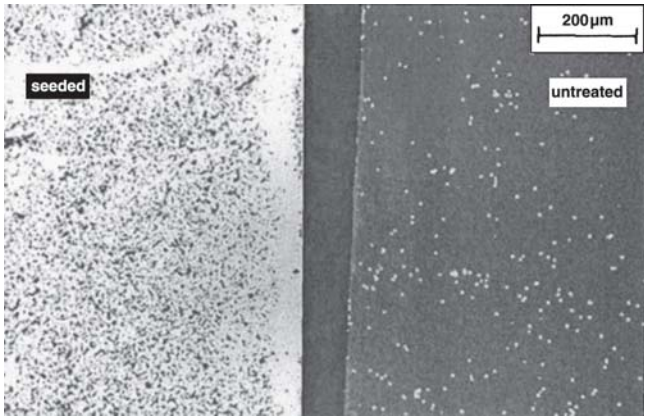

Fig. 3 Different diamond nucleation on seeded (left) and unseeded (right) nc70 interlayers after 4 h of CVD

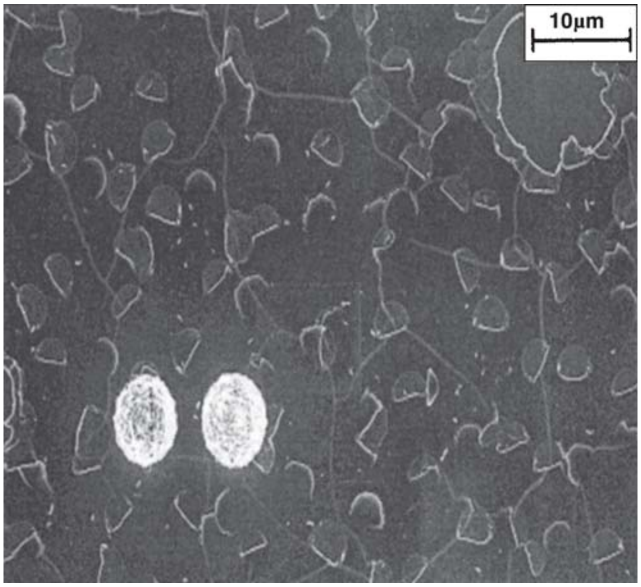

Fig. 4 Delamination of the low-temperature (70 °C) nc interlayer after diamond CVD

3.2 Nc400

Figure 5 shows that the preliminary seeding treatment of the TiN/SiN$_x$ layer had a positive effect on diamond nucleation in the case of nc films deposited at the higher temperature. There were some areas on the substrate where the deposition of the nc film did not occur, and only Si was present even though the entire substrate was immersed in the diamond suspension. It is worth noting that diamond nucleation on bare Si was significantly lower than on TiN/SiN$_x$, which is clearly visible in Fig. 6. Diamond nucleation is related to the carbon solubility and carbon diffusivity into the substrate (Ref 20), which in turn determines the surface carbon concentration and supersaturation (Ref 21). The larger number of diamond nuclei formed under the same CVD conditions as on the TiN/SiN$_x$ with re-

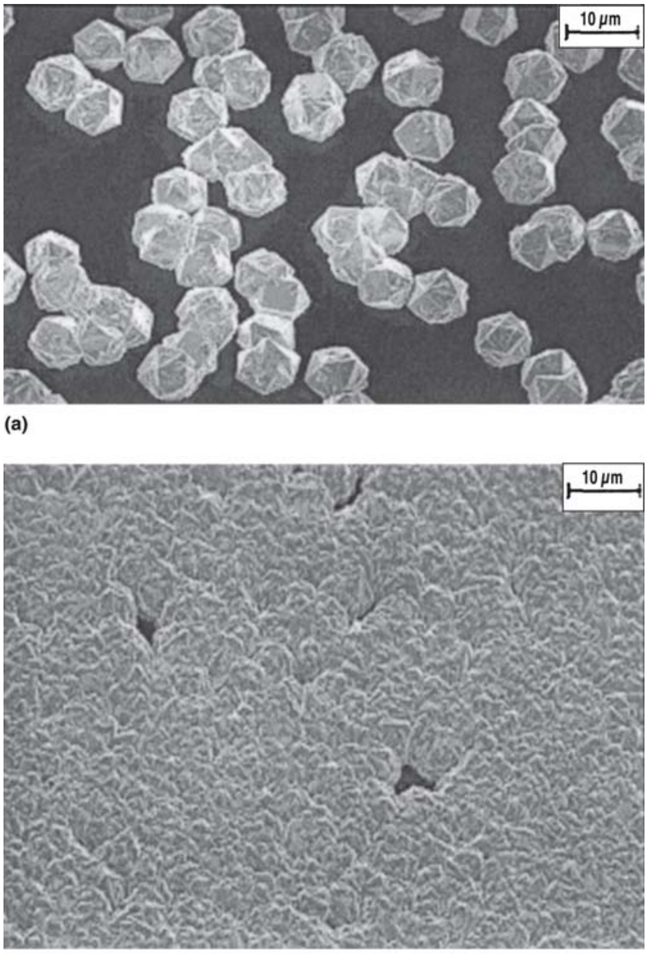

(a)

(b)

Fig. 5 SEM micrographs of the diamond deposit formed after 4 h of CVD on (a) seeded and (b) unseeded nc400 interlayers

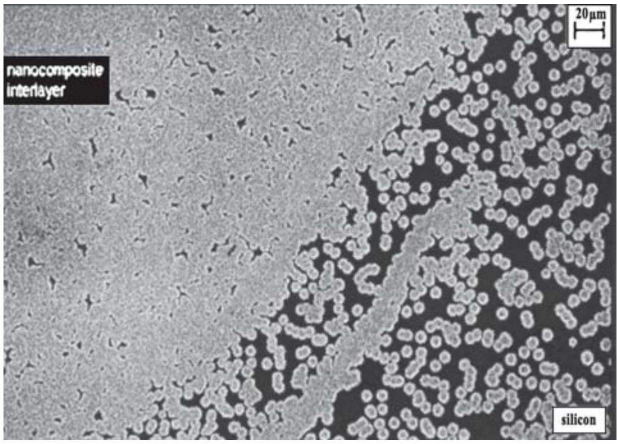

Fig. 6 SEM micrograph showing the effect of seeding on the diamond nucleation density at the bare surface and at the TiN/SiN$_x$ coated surface of the same silicon substrate. The nc layer was deposited at 400 °C.

spect to bare Si, which dissolves carbon and forms silicon carbide. This suggests that nc materials could act as an effective buffer layer for carbon diffusion, limiting interaction with the substrate.

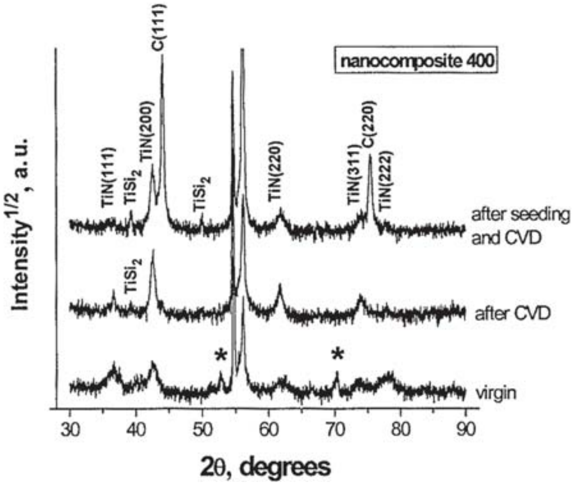

Fig. 7 Low-angle XRD spectra of nc films grown on sc-Si at 400 °C before (virgin) and after diamond CVD

Figure 7 shows the XRD spectra of both virgin and diamond CVD nc400 samples. Again, the presence of TiN, with a lattice parameter of approximately 0.425 nm, was evident. Moreover, peaks attributable to the substrate at $2\theta = 55°$ and two unidentified peaks (marked with an asterisk in Fig. 7) at $2\theta = 52.7$ and 70.2°, were present. However, the XRD pattern of TiN nanocrystals in the virgin TiN/SiN$_x$ nc coating prepared at 400 °C showed different features with respect to the nc70 sample. In fact, the TiN (200) reflection was now clearly visible in the XRD pattern, although at a lower intensity than the (111) peak. In fact, the measured intensity ratio, I_{200}/I_{111}, was 0.81 instead of 1.39 (JCPDS card No. 38-1420) (Ref 18). This fact suggests that a slight (111) preferential orientation of TiN nanocrystals was present, but much less pronounced than the one in nc films obtained at 70 °C. The FWHM of the (111) and (200) peaks gave an average TiN nanocrystals size of 16 ± 4 nm. After diamond CVD, independent of a preliminary seeding treatment, the texture of TiN nanocrystals changed to a predominant (100) orientation. In fact, for different samples, the ratio of the integrated intensity of the (200) peak over the total integrated intensity of all other TiN peaks in the 2θ range from 30° to 90° was 1.4 ± 0.3, i.e., about twice the value corresponding to randomly oriented crystallites (0.68). Also different from nc70 samples, the average size of TiN particles, determined by the FWHM of (111) and (200) TiN peaks, increased to 50 ± 7 nm during diamond CVD. Their growth was also assessed by SEM observation. In fact, the SEM morphology of as-prepared nc400 layers was not significantly different from that of the TiN/SiN$_x$ film deposited at the lower temperature (nc70, Fig. 1). However, after diamond CVD the size of TiN particles detectable by high-resolution SEM was significantly larger. Figure 8 shows the secondary electrons image of the surface of the unseeded nc-coated substrate after 4 h of diamond CVD. The dimensions of the TiN particles agreed well with the average crystallite size value estimated from XRD data.

The XRD spectra of the samples subjected to diamond CVD also showed weak peaks attributable to TiSi$_2$ (JCPDS card No. 85-879) (Ref 22), which were more intense for the seeded substrates (Fig. 7). Amorphous TiSi$_2$ could be present in Ti-Si-N nc materials, and its presence was verified by x-ray photoelectron spectroscopy (Ref 13). Nanocrystalline (detectable by XRD) TiSi$_2$ can precipitate at larger Si contents (>10 at.%),

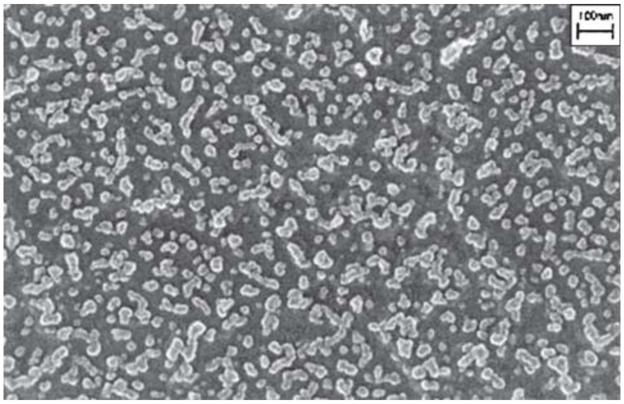

Fig. 8 SEM micrograph showing the morphology of TiN particles (bright phase) after diamond CVD on unseeded nc400 layer

as shown by Vepřek et al. (Ref 13). However, because crystalline or nanocrystalline $TiSi_2$ was not detected in the virgin nc coatings, its formation could be associated with the diffusion processes in the nc400 layers, which led to TiN particle growth and the crystallization of $TiSi_2$.

4. Conclusions

Thin (0.2 μm) TiN/SiN_x coatings have been prepared at 70 and 400 °C to investigate their potential use as interlayers for high-temperature diamond CVD on hostile substrates. XRD and SEM characterization showed that these materials were formed of amorphous silicon nitride with TiN crystallites of about 10 to 20 nm. Nc layers deposited at the lower temperature underwent minor changes in the nanostructure, but they delaminated during diamond CVD due to the large TEC mismatch at the two deposition temperatures (70 and 700 °C). The nc coatings deposited at the higher temperature underwent major changes in structure during diamond CVD, namely, TiN grain growth. It is well established that hardness enhancement arises from nanostructural conditions and by maintaining the TiN particle size as small as possible. Therefore, it is quite easy to predict that the hardness of nc coatings prepared at 400 °C would drop during diamond CVD. However, their use as interlayers in this case acts as a barrier to carbon diffusion, rather than as a wear-reducing coating. The nanostructural changes exhibited by nc coatings deposited at 400 °C were canceled by the absence of any visible delamination during diamond CVD and by larger nucleation densities compared with bare Si substrates subjected to the same seeding treatments prior to CVD. Therefore, nc coatings are promising materials for use as interlayers for diamond deposition onto hostile substrates, provided the deposition temperature is as close as possible to the temperature of diamond CVD. These results have led to a deposition approach that could potentially serve as an exceptional interlayer for film deposition onto steel and WC-Co. Preliminary tests on nc interlayers deposited at 400 °C are in progress.

References

1. R.F. Davis, Ed., *Diamond Films and Coatings*, Noyes Publications, Park Ridge, NJ, 1993
2. R. Haubner, A. Lindlbauer, and B. Lux, Diamond Deposition on Chromium, Cobalt and Nickel Substrates by Microwave Plasma Chemical Vapour Deposition, *Diamond Relat. Mater.,* 1993, **2,** p 1505-1515
3. M. Nesládek, K. Vandierendonck, C. Quaeyhaegens, M. Kerkhofs, and L.M. Stals, Adhesion of Diamond Coatings on Cemented Carbides, *Thin Solid Films,* 1995, **270,** p 184-188
4. A. Inspektor, E.J. Oles, and C.E. Bauer, Theory and Practice in Diamond Coated Metal-Cutting Tools, *Int. J. Refract. Met. Hard Mater.,* 1997, **15,** p 49-56
5. H.-J. Jentsch, G. Rosenbauer, S.M. Rosiwal, and R.F. Singer, Graphite Interlayer Formation During CVD Diamond Coating of Iron Base Alloys, *Adv. Eng. Mater.,* 2000, **2,** p 369-374
6. S. Schwarz, S.M. Rosiwal, Y. Musayev, and R.F. Singer, High Temperature Diffusion Chromizing as a Successful Method for CVD-Diamond Coating of Steel—Part II, *Diamond Relat. Mater.,* 2003, **12,** p 701-706
7. X. Chen and J. Narayan, Effect of the Chemical Nature of Transition-Metal Substrates on Chemical-Vapor Deposition of Diamond, *J. Appl. Phys.,* 1993, **74,** p 4168-4173
8. S. Silva, V.P. Mammana, M.C. Salvadori, O.R. Monteiro, and I.G. Brown, WC-Co Cutting Tool Inserts with Diamond Coatings, *Diamond Relat. Mater.,* 1999, **8,** p 1913-1918
9. W.D. Fan, X. Chen, K. Jagannadham, and J. Narayan, Diamond-Ceramic Composite Tool Coatings, *J. Mater. Res.,* **9,** 1994, p 2850-2856
10. C. Faure, W. Hänni, C. Julia Schmutz, and M. Gervanoni, Diamond-Coated Tools, *Diamond Relat. Mater.,* 1999, **8,** p 830-833
11. I. Endler, A. Leonhardt, H.-J. Scheibe, and R. Born, Interlayers for Diamond Deposition on Tool Materials, *Diamond Relat. Mater.,* 1996, **5,** p 299-303
12. S. Li, Y. Shi, and H. Peng, Ti-Si-N Films Prepared by Plasma-Enhanced Chemical Vapor Deposition, *Plasma Chem. Plasma Process.,* 1992, **12,** p 287-297
13. S. Vepřek, A. Niederhofer, K. Moto, T. Bolom, H.-D. Männling, P. Nesladek, G. Dollinger, and A. Bergmaier, Composition, Nanostructure and Origin of the Ultrahardness in nc-TiN/a-Si_3N_4/a- and nc-$TiSi_2$ ncs with $H_V = 80$ to ≥105 GPa, *Surf. Coat. Technol.,* 2000, **133-134,** p 152-159
14. J.S. Colligon, Ion-Assisted Sputter Deposition (Sputtering: Past, Present and Future), *Philos. Trans. R. Soc. London,* 2004, **362,** p 103-116
15. S. Iijima, Y. Aikawa, and K. Baba, Growth of Diamond Particles in Chemical Vapour Deposition, *J. Mater. Res.,* 1991, **6,** p 1491-1503
16. E. Molinari, R. Polini, and M. Tomellini, Diamond Crystallite Formation on Si(100) from the Gas Phase, *Appl. Phys. Lett.,* 1992, **61,** p 1287-1289
17. E. Molinari, R. Polini, M.L. Terranova, P. Ascarelli, and S. Fontana, Uncoupling Crystal Growth and Nucleation in the Deposition of Diamond from the Gas Phase, *J. Mater. Res.,* 1992, **7,** p 1778-1783
18. JCPDS 38-1420, International Center for Powder Diffraction Data, Swarthmore, PA, 1989
19. L. Rebouta, C.J. Tavares, R. Aimo, Z. Wang, K. Pischow, E. Alves, T.C. Rojas, and J.A. Odriozola, Hard nc Ti-Si-N Coatings Prepared by DC Reactive Magnetron Sputtering, *Surf. Coat. Technol.,* 2000, **133-134,** p 234-239
20. H. Liu and D.S. Dandy, *Diamond Chemical Vapor Deposition—Nucleation and Early Growth Stages*, Noyes Publications, Park Ridge, NJ, 1995
21. Y. Mitsuda, T. Moriyasu, and N. Masuko, Effect of High Supersaturation at the Initial Stage on Diamond Nucleation Phenomena, *Diamond Relat. Mater.,* 1993, **2,** p 333-336
22. JCPDS 85-879, International Center for Powder Diffraction Data, Swarthmore, PA, 1989